The uSed System for Soil Particle Size Distribution Determination

Lei Zhang, S.M.ASCE¹; Roman D. Hryciw, Ph.D., M.ASCE²; and Andrea Ventola, Ph.D., M.ASCE³

¹Dept. of Civil and Environmental Engineering, Univ. of Michigan, Ann Arbor, MI.

Email: leileizh@umich.edu

²Dept. of Civil and Environmental Engineering, Univ. of Michigan, Ann Arbor, MI.

Email: romanh@umich.edu

³Dept. of Civil and Environmental Engineering, Univ. of Michigan, Ann Arbor, MI.

Email: acvent@umich.edu

ABSTRACT

A new testing system for determining soil particle size distributions (PSDs) is under development. It augments existing systems generically called "SedImaging" by the addition of a water pressure transducer near the bottom of a soil sedimentation column. The original SedImaging test provides image-based PSDs for sands, while the pressure transducer will extend the PSDs into the silt range. The new test system is called the "uSed" reflecting the measurement of water pressures (u) during a SedImaging test. This paper presents the uSed theoretical equations and the results of four pilot tests on sands to verify the theory. The four specimens were coarse sand, medium-sized sand, fine sand, and a gap-graded sand. The observed pressure decay curves were qualitatively as expected and the masses of solids predicted by the uSed theory agreed with the actual specimen masses to within an error of 2%.

INTRODUCTION

Particle size distributions (PSDs) are valuable first indicators of fundamental mechanical and geohydrologic soil properties such as compressibility, shear strength, and hydraulic conductivity (Sun et al. 2015; Bodman and Constantin 1965; Wang et al. 2013; Wang et al. 2019; Ahmed et al. 2023). Traditionally, a soil specimen's PSD is determined by sieving. However, as discussed by Ohm et al. (2013), sieving is time consuming, energy intensive, and costly. Therefore, a rapid, energy-efficient, low-noise method called SedImaging was developed by Ohm and Hryciw (2014) to optically determine a sand specimen's PSD. A field-adaptable version of the system called FieldSed was developed by Ventola et al. (2019) to determine the PSDs of many soil specimens concurrently. Subsequently, an automated version called Sed360 expanded test utilization to the full range of sand particle sizes (Ventola and Hryciw 2023a). All of the SedImaging versions utilize sedimentation of a soil through a tall water column to sort the particles by size prior to photographing the accumulated specimen at the column base. The image analysis, which is based on the mathematical Harr Wavelet Transform (HWT), has been described by Hryciw et al. (2015) and Ventola and Hryciw (2023b).

Due to field-of-view and image magnification constraints, the testable size range for all previous SedImaging systems was limited to particles larger than 0.075 mm (No. 200 sieve). To overcome this limitation, a new SedImaging system called "uSed" (pronounced "you-said") is being developed which will extend the viable testing size range to particles smaller than 0.075 mm. The uSed system adds a water pressure transducer near the bottom of the sedimentation

column to record the pressure generated by the soil particles and water above the pressure port during sedimentation. From the pressure time histories, the weight of solids that are still above the pressure port elevation at any time can be calculated. Eventually, a high magnification camera will be used to determine the sizes of the particles passing the pressure port with time. This will yield a weight-based PSD for the soil. Image analysis is still utilized on the sand fraction of a uSed specimen.

This paper presents the uSed hardware, theory, typical pressure time histories, and the results of four tests as proof of the uSed concept. The paper does not cover the image analysis aspects of the uSed system. Although the uSed aims to extend PSD determination into the silt range, the test results presented herein will be for various gradations of sands. This is only because sand specimens are easier to prepare, handle and test.

THE USED SYSTEM

The uSed system is shown in Fig. 1. It consists of a 1.8 m (6 ft) long clear acrylic sedimentation column with a 25.4 mm (1 in) diameter opening and a 3.2 mm (1/8 in) wall thickness. The column is open on the top, and sits on a detachable acrylic pedestal base. Figure 1 also shows a mounted Nikon D800 DSLR camera. The uSed sedimentation column and its pedestal base sit on a load transfer system and a Thorlabs precision rotation stage. These hardware features are described in detail by Ventola and Hryciw (2023a) and are not critical to the uSed research topics covered in this paper.

The new hardware for the uSed system includes a pressure transducer with a measuring range of 0 to 30 kPa. It was custom-made by the Chaoyuan Instrument Factory in China. The model number is UYY-30kPa. Importantly, the transducer assembly contains a vent hole for bleeding trapped air from the tubing and transducer chamber to insure saturation in the line. The tubing is connected to a pressure port located 20 cm (7.9 in.) above the base of the sedimentation column. This port elevation was established to ensure that it will be above the top of the final settled soil specimen. A typical 100 g settled specimen is about 15 cm (5.9 in.) tall. The port on the column has a 9.53 mm (3/8 in) diameter and is connected to the pressure transducer by plastic tubing of the same diameter with a push-to-connect fitting. The fitting is open when the tube is inserted and automatically closes to seal the system when the tubing is removed. A drainage port (Fig. 1) is located on the pedestal base. It is used to introduce distilled water into the sedimentation column and to drain the column after a test.

PERFORMING A USED TEST

To perform a uSed test, the pressure port is connected to the transducer and the pressure data acquisition begins. Pressure readings are gathered every 1/10 of a second with a known accuracy of ± 5.15 Pa. Next, the sedimentation column is filled with room temperature distilled water via the drainage port. A uSed soil specimen is introduced into the open top of the water-filled sedimentation column. Once released, the soil particles immediately begin to settle through the column and eventually accumulate at the base. Larger soil particles settle first, with progressively finer soil particles settling overtop. After the entire soil specimen has settled at the base of the sedimentation column, the pressure data acquisition ends. At this stage, the tubing is removed and the settled soil specimen can be photographed. The soil images can be analyzed following the same procedure used for the Sed360, as described by Ventola and Hryciw (2023a). Once testing is complete, the column is drained and detached from the pedestal base for cleanup.

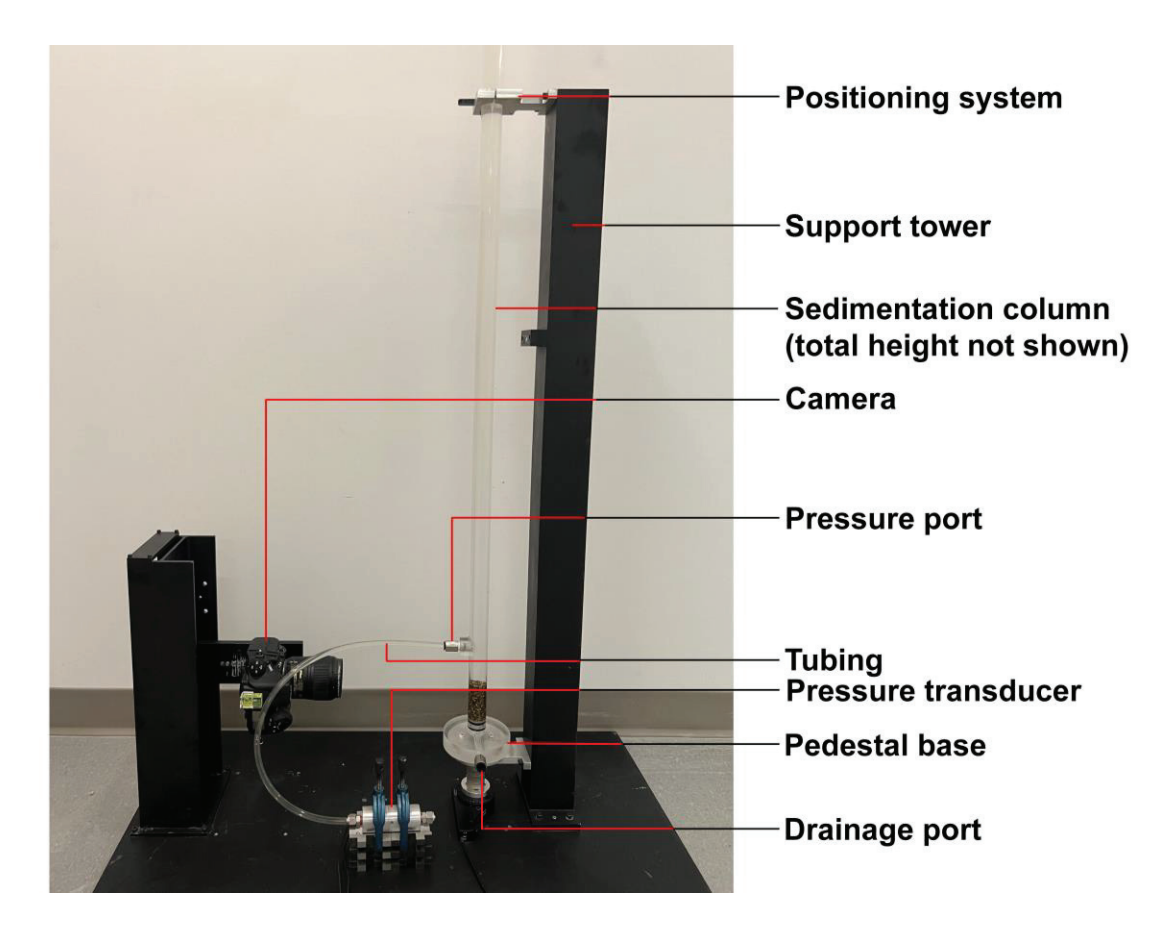


Figure 1. The uSed system.

The transducer records the pressure due to all of the water and soil that is above the pressure port elevation. Pressure readings are gathered during the entire uSed test, from filling the sedimentation column with distilled water, during introduction of a soil specimen into the top of the column, and throughout the sedimentation process. As will be shown next, the recorded pressure time-history can be used to (1) determine the overall weight of a soil specimen and (2) differentiate particle sizes in a soil specimen. Future research will combine this information with image analysis methods to determine the particle size distribution of sands and, for the first time with SedImaging, silts.

USED PRESSURE READINGS

The upper portion of Figure 2 is a visual representation of a soil specimen's sedimentation through the uSed column at eight moments in time. The bottom of the figure shows the expected pressure trends corresponding to these times. The uSed pressure readings occur over six stages, labeled A through F in Fig. 2. In Stage A, distilled water is introduced into the sedimentation column through the drainage port (Fig. 1). The slope of the pressure reading versus time data in Stage A is a function of the unit weight of the water and the speed of its introduction into the column. Once filling with water is complete, the uSed pressure readings remain constant during Stage B. During Stage C, soil particles are introduced into the top of the sedimentation column. The slope of the pressure versus time readings in Stage C is a function of the weight of the soil and the speed at which it is added into the column.

After a specimen's introduction, soil particles immediately begin to settle through the water. Coarser soil particles settle faster than finer particles. While the entire settling soil specimen remains above the pressure port, pressure readings remain constant (Stage D). Stage E occurs when soil particles are passing the elevation of the port. During this stage, pressure readings decrease with time. After the last soil particles settle below the port, the pressure readings will once again become constant (Stage F). Since the soil introduction into the sedimentation column causes an increase in the water level, the constant pressure readings in Stage F are higher than during Stage B as illustrated by a dashed horizontal line in Fig. 2.

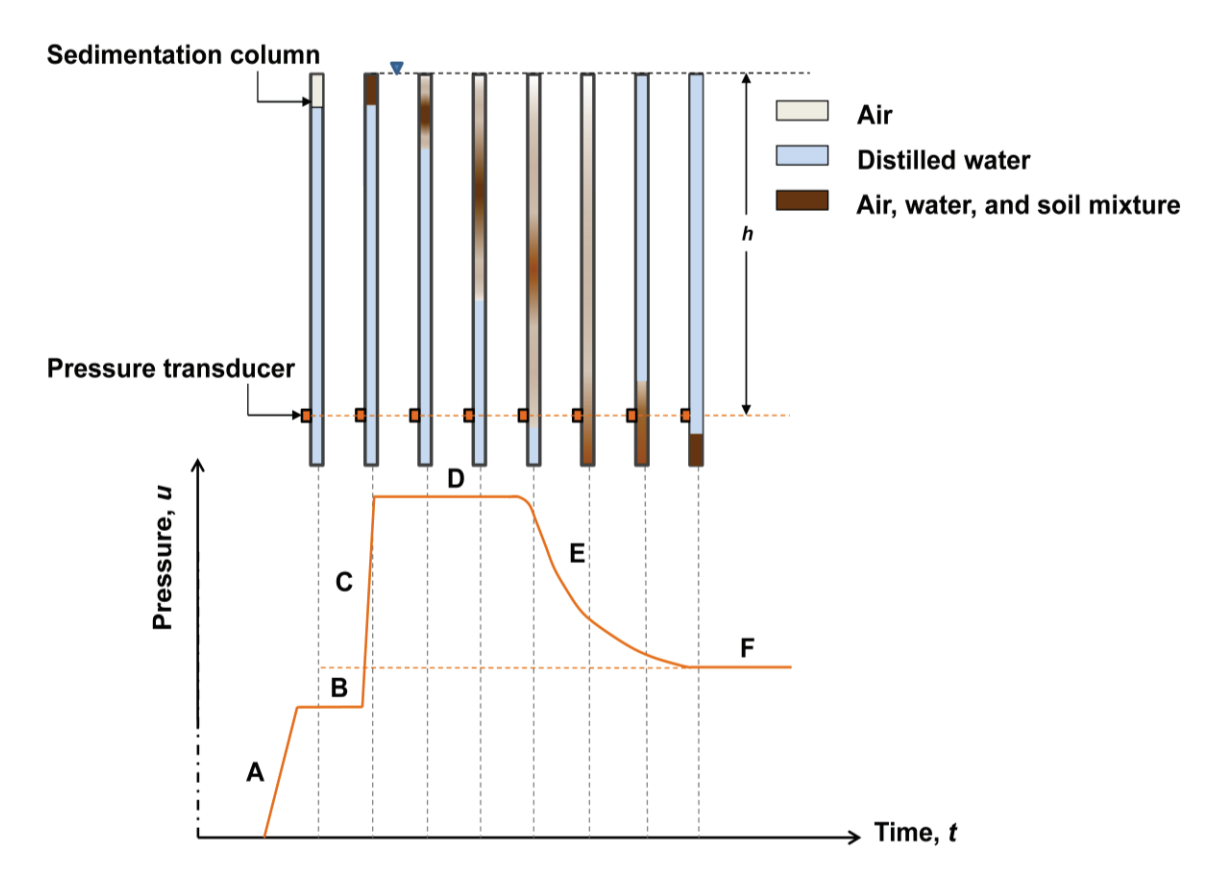


Figure 2. Theoretical pressure reading stages during a uSed test.

The rate of pressure decrease during Stage E is related to the settling velocity and weight concentration of particles passing the pressure port. Coarser particles naturally settle faster than finer ones. Therefore, for similar weight concentrations, their passage past the port will result in a faster pressure decrease than finer particles will during Stage E.

Governing uSed Equations

During the uSed test, pressure readings are used to calculate the weight of solids (soil particles) that are above the elevation of the pressure port as a function of time. To do so, the pressures during Stages D, E, and F of Fig. 2 are used. During Stage D, the particles are already in the water column and are settling and sorting, but none have yet passed the pressure port. During this stage, the water pressure at the elevation of the pressure port is constant and given by:

$$u^D = \frac{W_s + W_w^D}{A} \tag{1}$$

where u^D = constant pressure during Stage D

 W_s = total weight of solids

 W_w^D = weight of water above the pressure port elevation during Stage D

A =inside cross-sectional area of the sedimentation column.

The weights of solids and water in Eq. (1) can be expressed in terms of their respective volumes:

$$u^{D} = \frac{V_s G_s \gamma_w + V_{aw}^D \gamma_{aw}}{A} \tag{2}$$

where V_s = volume of solids

 G_s = specific gravity of solids

 γ_w = unit weight of water at 4 °C = 9.81 kN/m³.

Recognizing that air bubbles could be present in the column, the authors use:

 V_{aw}^{D} = volume of air-water mixture above the pressure port during Stage D

 γ_{aw} = unit weight of air-water mixture.

Equation (2) may also be written:

$$u^{D} = \frac{V_s G_s \gamma_w + (V - V_s) \gamma_{aw}}{A} \tag{3}$$

where V = hA

h = height of water in the column above the pressure port (see Figure 2).

Equation (3) is reorganized as:

$$u^{D} = \frac{V_s(G_s \gamma_w - \gamma_{aw})}{A} + h\gamma_{aw}$$
 (4)

During Stage E, particles are passing the pressure port, the volume of solids above the port is decreasing, and the pressure is decreasing. During this stage, Eq. (4) becomes:

$$u^{E} = \frac{V_s^{E}(G_s \gamma_w - \gamma_{aw})}{A} + h\gamma_{aw}$$
 (5)

where u^E = pressure during Stage E

 V_s^E = volume of solids above the pressure port during Stage E.

Subtracting Eq. (5) from Eq. (4) we obtain:

$$u^{D} - u^{E} = (V_s - V_s^{E}) \frac{G_s \gamma_w - \gamma_{aw}}{A}$$
 (6)

Equation (6) is solved for the volume of solids above the pressure port:

$$V_s^E = V_s - \frac{(u^D - u^E)A}{G_s \gamma_w - \gamma_{aw}} \tag{7}$$

Alternatively, the volume of solids that have passed the pressure port can be computed:

$$V_s - V_s^E = \frac{(u^D - u^E)A}{G_s \gamma_w - \gamma_{aw}}$$
(8)

The related weight of solids that have passed the pressure port is then:

$$W_s - W_s^E = \frac{(u^D - u^E)AG_s\gamma_w}{G_s\gamma_w - \gamma_{gw}}$$
(9)

where W_s^E = weight of solids above the pressure port during Stage E.

Finally, during Stage F, all of the soil particles have passed the pressure port and thus, $W_s^E = 0$. The total weight of solids in the specimen is therfore:

$$W_s = \frac{(u^D - u^F)AG_s\gamma_w}{G_s\gamma_w - \gamma_{aw}} \tag{10}$$

where u^F = constant pressure during Stage F.

The ratio of Eq. (9) to Eq. (10) x 100 is the percentage of specimen solids that have settled past the pressure port at any time during Stage E. A high magnification camera will eventually be used to determine the size of silt particles passing the pressure port with time. Thus, a weight-based PSD for the soil will be obtained.

RESULTS

Four uSed tests were performed to validate the uSed theory. The tests were also used to observe how particle size controls the rate of pressure decay in Stage E. Table 1 lists the four uSed specimens, which include a coarse sand (Specimen 1), medium sand (Specimen 2), fine sand (Specimen 3), and gap-graded sand (Specimen 4). Specimen 4 was created using equal parts coarse and fine sand. The soil is a glacio-fluvial sand known as "2NS" by the Michigan Department of Transportation (MDOT) (MDOT 2010). To create the four specimens, 2NS was sieved into narrow size ranges according to ASTM C136/C136M-19 (ASTM 2019). The specific gravity, G_s (ASTM 2016) of 2NS is 2.66. The four uSed tests were conducted using distilled water that was allowed to reach an ambient temperature of 25°C (77°F) prior to testing. The unit weight of the system's distilled water (γ_{aw}) was determined to be 9.77 kN/m^3 , which means that some air was present. This unit weight is assumed to remain constant throughout each of the four tests.

Specimen No.	U.S. Sieve Range	Particle Size Range (mm)	Sand Classification ^a	Duration of Stage D (s)	Specimen Mass by uSed (Eq. 10) (g)	Actual Specimen Mass (g)
1	No. 6 – No. 8	3.35 - 2.36	Coarse	4.3	60.75	60.00
2	No. 18 – No. 25	1.00 - 0.71	Medium	6.1	60.33	60.00
3	No. 40 – No. 50	0.425 - 0.30	Fine	13.1	59.47	60.00
4	No. 6 – No. 8	3.35 - 2.36	Coarse	4.2	30.60	30.00
	No. 40 – No. 50	0.425 - 0.30	Fine		29.73	30.00

Table 1. uSed test results.

Figure 3 presents the uSed pressure readings for the fine sand (Specimen 3). Labeled within Fig. 3 are the same stages of pressure readings as described in Fig. 2 (Stage A is omitted in Fig. 3 to enhance the resolution of Stages B through F). As anticipated, the actual pressure stages in Fig. 3 are consistent with the six expected stages from Fig. 2.

The pressure readings of the four specimens during Stages D, E and F are plotted in Fig. 4. The start of Stage D is set to t=0 seconds for discussion purposes. As expected, the fine sand (Specimen 3) has the longest Stage D duration (13.1 seconds), followed by the medium sand (Specimen 2) with 6.1 seconds. The coarse sand (Specimen 1) and the gap-graded sand (Specimen 4) have the shortest, and nearly identical, Stage D durations (4.3 and 4.2 seconds respectively). Settling velocity through water increases with particle size, which results in coarser sands reaching the elevation of the pressure port quicker (i.e. a shorter Stage D) than finer sands. The coarse and gap-graded sands have similar time periods for Stage D because of the identical size of their coarse particles (2.36mm to 3.35mm diameter). The gap-graded's fine sand portion does not affect the timing of the specimen's Stage D but it *does* affect the duration (i.e. the pressure reading decay) of Stage E. As expected, the rate of pressure decrease during Stage E is a function of the settling velocities and weight concentrations of soil particles passing the elevation of the pressure port. Of the four specimens, the coarse sand (Specimen 1) has the steepest slope, followed by the medium sand (Specimen 2). The slowest decay of Stage E readings is for the fine sand (Specimen 3).

The gap-graded sand (Specimen 4) has a unique Stage E pressure decay. After its release into the sedimentation column, the gap-graded specimen's coarse and fine sand particles naturally became sorted by size. All of the coarse sand particles settled past the pressure port before 9.4 seconds, which is why the gap-graded's pressure decay is nearly identical to that of the coarse sand (Specimen 1) before t = 9.4 seconds. During the subsequent constant pressure phase, all of the gap-graded's fine sand is still settling through the water column, but it is all above the pressure port. Eventually, at time t = 12.6 s, the fine sand reaches the pressure port and begins to settle past it. If scaled vertically 2X to account for having only 30 g of fine sand rather than 60 g as Specimen 3 did, the gap-graded sand's Stage E pressure decay is essentially the same as that of the fine sand beyond 12.6 seconds. The pressure readings of the gap-graded sand confirm the natural sorting of sand by particle size during sedimentation and validates the expected uSed pressure time histories.

The mass of each sand specimen calculated from the uSed pressure readings according to Eq. 10 is listed in Table 1. These values are compared to the specimens' actual masses (60.00 g). For all four tests, the soil mass computed using the uSed is close to the specimens' actual mass (all

^a According to the Unified Soil Classification System (USCS)

errors are 2% or less), which confirms the reliability of the uSed testing system for determining specimen mass.

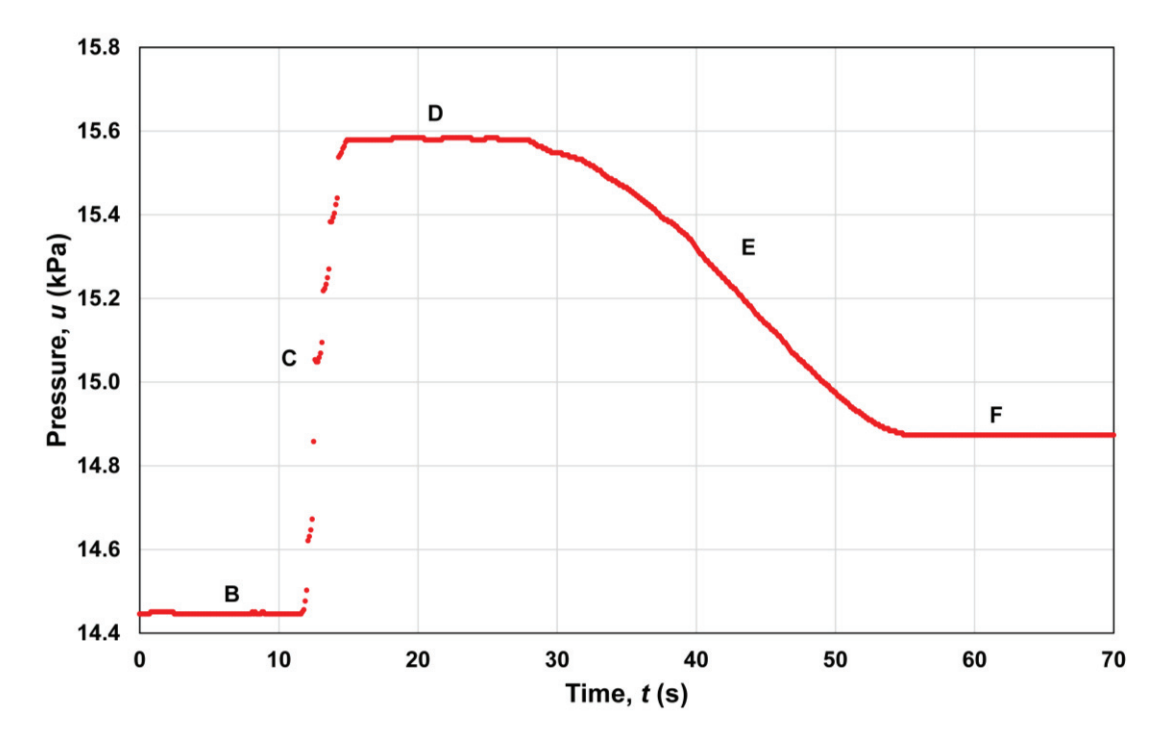


Figure 3. Fine sand (Specimen 3, No. 40 – No. 50 sieves) uSed pressure readings.

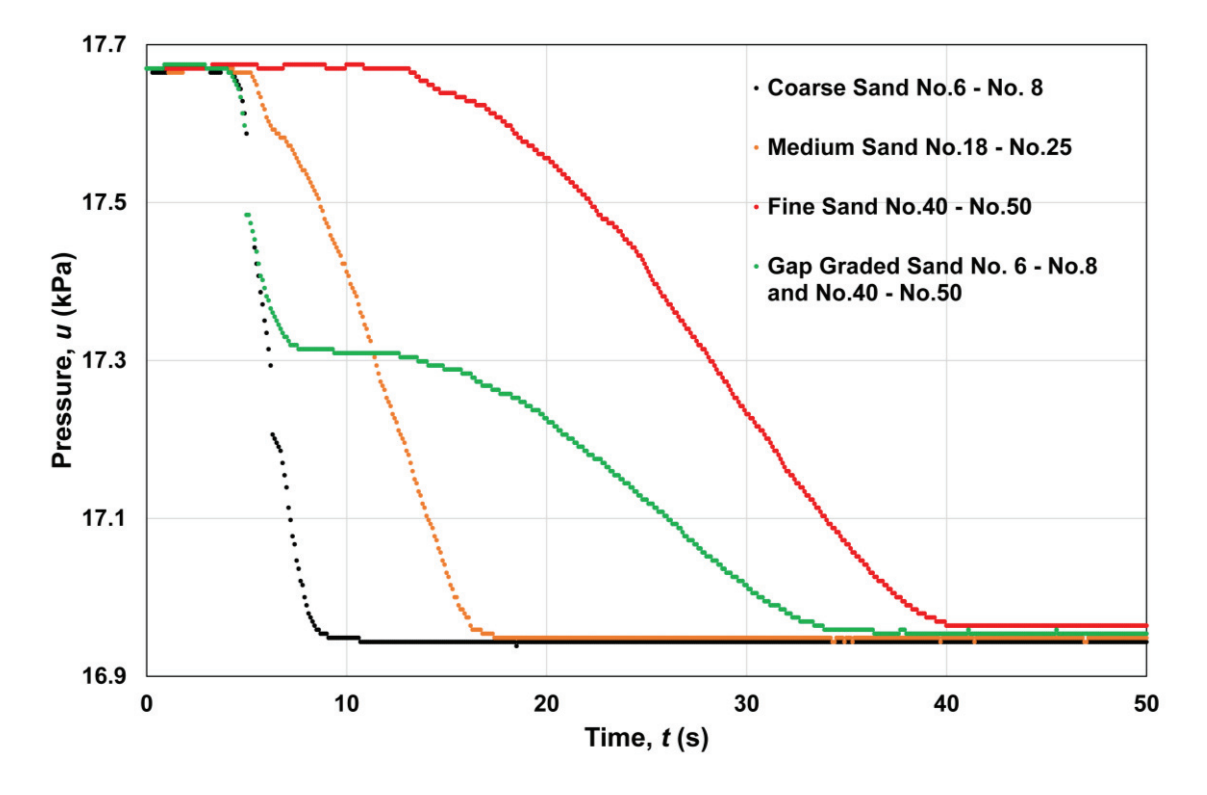


Figure 4. Comparison of pressure readings for the four uSed specimens.

DISCUSSION

As seen in Table 1, the uSed tends to slightly overpredict the mass of coarser sand (Specimen 1, 2, and the coarse portion of Specimen 4) while it tends to slightly underpredict the mass of finer sand (Specimen 3 and the fine portion of Specimen 4). The authors believe the overprediction of coarser particle weights is related to the effect of acceleration before the soil particles reach a constant settling velocity. When comparing the results of coarse sand (Specimen 1) and medium sand (Specimen 2), although the total soil weight of both is overpredicted, the overprediction for coarse sand is greater.

Regarding the underpredicted mass of the fine sands, the authors suspect that due to electrostatic attractions, some fine sand particles adhere to the inner wall of the sedimentation column. Particles that adhere to the inner wall do not contribute to the pressure readings, which leads to an underprediction of the weight of the fine sand by the uSed system. More research is needed to verify these possible explanations for over- and underpredicted specimen masses.

Lastly, this paper described only half of the uSed system. It presents the research associated with measuring water pressure to determine the percentage of solids above the pressure port at any instant in time. By analogy, this is like describing a hydrometer without discussing Stokes' Law (which is needed to determine the particle sizes still in suspension at any instant in time during a hydrometer test). The natural inclination would be to invoke Stokes' Law in the uSed test as well. The reason for not doing so is that the high concentration of sedimenting solids in the uSed test lowers the settling velocities of particles. This occurs because of the upward flow of water being displaced by the falling solids. Stokes' Law is invalid under these conditions. Instead, the authors plan to utilize a microscope-camera system to detect the size of particles as they pass the level of the pressure port. Such an optical technique may be able to size silt-sized particles, but certainly not clays. Thus, a hybrid combination of pressure readings and optical methods may eventually be developed. The use of a microscope-camera is not to be confused with the conventional DSLR camera system (Fig. 1) that is used for characterizing the sand-size fractions of soil specimens in SedImaging.

CONCLUSIONS

A new uSed system is being developed to extend the viable testing size range of SedImaging to include soil particles smaller than 0.075 mm. During particle sedimentation, a pressure transducer records the pressure generated by a soil specimen and the water above a pressure port located near the base of the system's water column. The weight of solids above the pressure port elevation can be obtained from the pressure readings. The results of four sands tested in the uSed match the expected pressure reading trends. Agreement (≤2% error) is also seen between the specimen's known masses and their calculated masses using the uSed pressure readings.

ACKNOWLEDGEMENTS

This material in this paper is based upon work supported by the US National Science Foundation under Grant CMMI 1825189. ConeTec Investigations Ltd. and the ConeTec Education Foundation are acknowledged for their support to the Geotechnical Engineering Laboratories at the University of Michigan. The authors thank Steve Donajkowski and Ethan Kennedy for providing design suggestions and machining for the uSed.

REFERENCES

- Ahmed, S. S., Martinez, A., and DeJong, J. T. (2023). "Effect of gradation on the strength and stress-dilation behavior of coarse-grained soils in drained and undrained triaxial compression." *Journal of Geotechnical and Geoenvironmental Engineering*, 149(5): 04023019.
- ASTM. (2016). Standard Test Methods for Specific Gravity of Soil Solids by Water Pycnometer. ASTM D854-14 West Conshohocken, PA.
- ASTM. (2019). Standard Test Method for Sieve Analysis of Fine and Coarse Aggregates. ASTM C136/C136M-19, West Conshohocken, PA.
- MDOT (Michigan Department of Transportation). (2010). *Materials Source Guide*. 902, 200 Lansing, MI.
- Bodman, G. B., and Constantin, G. K. (1965). "Influence of particle size distribution in soil compaction". *Hilgardia*, 36(15): 567–591.
- Hryciw, R. D., Ohm, H.-S., and Zhou, J. (2015). "Theoretical basis for optical granulometry by wavelet transformation." *Journal of Computing in Civil Engineering*, 29(3): 1-10.
- Ohm, H.-S., and Hryciw, R. D. (2014). "Size distribution of coarse-grained soil by SedImaging." *Journal of Geotechnical and Geoenvironmental Engineering*, 140(4): 1-9.
- Ohm, H.-S., Sahadewa, A., Hryciw, R. D., Zekkos, D., and Brant, N. (2013). "Sustainable soil particle size characterization through image analysis." *Geotechnical and Geological Engineering*, 31(6): 1647–1652.
- Sun, Y., Xiao, Y., and Hanif, K. F. (2015). "Compressibility dependence on grain size distribution and relative density in sands." *Science China Technological Sciences*, 58(3): 443–448.
- Ventola, A., and Hryciw, R. D. (2019). "On-site particle size distribution by FieldSed." In *Geo-Congress 2019: Engineering Geology, Site Characterization, and Geophysics* (143-151). Reston, VA: ASCE.
- Ventola, A., and Hryciw, R. D. (2023a). "The Sed360 test for rapid sand particle size distribution determination." *Geotechnical Testing Journal*, 46(2): 422-429.
- Ventola, A., and Hryciw, R. D. (2023b). "An autoadaptive Haar wavelet transform method for particle size analysis of sands." *Acta Geotechnica*, 1-18.
- Wang, H.-L., Zhou, W.-H., Yin, Z.-Y., and Jie, X.-X. (2019). "Effect of grain size distribution of sandy soil on shearing behaviors at soil–structure interface." *Journal of Materials in Civil Engineering*, 31(10):04019238.
- Wang, J.-J., Zhang, H.-P., Tang, S.-C., and Liang, Y. (2013). "Effects of particle size distribution on shear strength of accumulation soil." *Journal of Geotechnical and Geoenvironmental Engineering*, 139(11): 1994–1997.